Hindawi Publishing Corporation
Journal of Nanomaterials
Volume 2012, Article ID 327583, 7 pages
doi:10.1155/2012/327583

Research Article

Making Organic-Inorganic Nanocomposites via Selective Dispersion of PS-Tethered SiO_2 Particles in Polystyrene-*Block*-Polymethylmethacrylate Copolymer

Chia-Hong Liu, Li-Ko Chiu, Je-Yuan Yeh, and Raymond Chien-Chao Tsiang

Department of Chemical Engineering, National Chung Cheng University, Chiayi 621, Taiwan

Correspondence should be addressed to Raymond Chien-Chao Tsiang, chmcct@ccu.edu.tw

Received 6 June 2011; Accepted 10 August 2011

Academic Editor: Hui Wang

SiO_2 nanoparticles have been dispersed selectively in the polystyrene (PS) microdomain of polystyrene-*block*-polymethylmethacrylate (PS-*b*-PMMA) block copolymer via the blending of PS-*b*-PMMA with PS-tethered SiO_2. As observed by atomic force microscopy and scanning electron microscopy, the incorporation of SiO_2 particles not only enlarges the PS microdomain but also reduces the surface energy of the PS microdomain and transforms the morphology from either lamellar layers or cylinders to islanded bicontinuous microstructures. Blending SiO_2 particles with an excessive amount or with a particle size larger than that of the PS microdomain would pose an extreme constraint on the molecular rearrangement, unstabliize the microdomain separation, and even make the microdomain separation unobservable. The nanosize and the uniform distribution of the PS microdomain in the PS-*b*-PMMA polymer have thus enabled us to achieve a uniform distribution of the inorganic SiO_2 particles in the organic polymeric matrix.

1. Introduction

Block copolymers are known for their microdomain separation which attains various periodic nanostructures under proper compositions and conditions [1–8]. In recent years, nanotemplating studies involving block copolymers have gained extensive interest. Nanowires such as Co, Ag, and Au or nanoparticles such as CdSe, Pd, and TiO_2 have been reported either to grow in or to be blended into a specific microdomain [9–15]. The selective dispersion of nanoparticles in one of the microdomains has great potential in applications such as photonic crystals with enhanced refractive index contrast between microdomains [9–11], and nanoporous hybrid membranes after etching one of the microdomains [16–34]. The growth of nanoparticles in one of the microdomains of a diblock copolymer often requires the functionalization of that specific microdomain with precursor complexes followed by an in situ reduction of that precursor complexes to form nanoparticles. On the other hand, the blending of nanoparticles into one of the microdomains requires the pretreatment of nanoparticles with various surfactants, such as ionic or nonionic types, or functioning agents containing functional groups compatible with the targeted microdomain.

Recently, it has been reported that blending a homopolymer hA into a block copolymer A-*b*-B would result in changes in the microdomain separation depending upon the temperature, the wt% of homopolymer, the molecular weight ratio of homopolymer to the corresponding block, and the overall volume ratio of constituting species [35–38]. Under proper conditions, homopolymer hA could be solubilized in the A block either locally or uniformly. These studies have prompted us to explore another approach to selectively disperse SiO_2 nanoparticles in a PS-*b*-PMMA diblock copolymer. Here, in the current study, we have synthesized two PS-*b*-PMMA diblock copolymers with different ratios of PS to PMMA block lengths, having either an alternating lamellar layers or cylindrical microstructures, as well as a trimethoxysilane-terminated homopolystyrene (PS-silane). This PS-silane was thereafter tethered to SiO_2 nanoparticles to form PS-SiO_2 particles, and these PS-SiO_2 particles were then blended quantitatively with PS-*b*-PMMA to make an

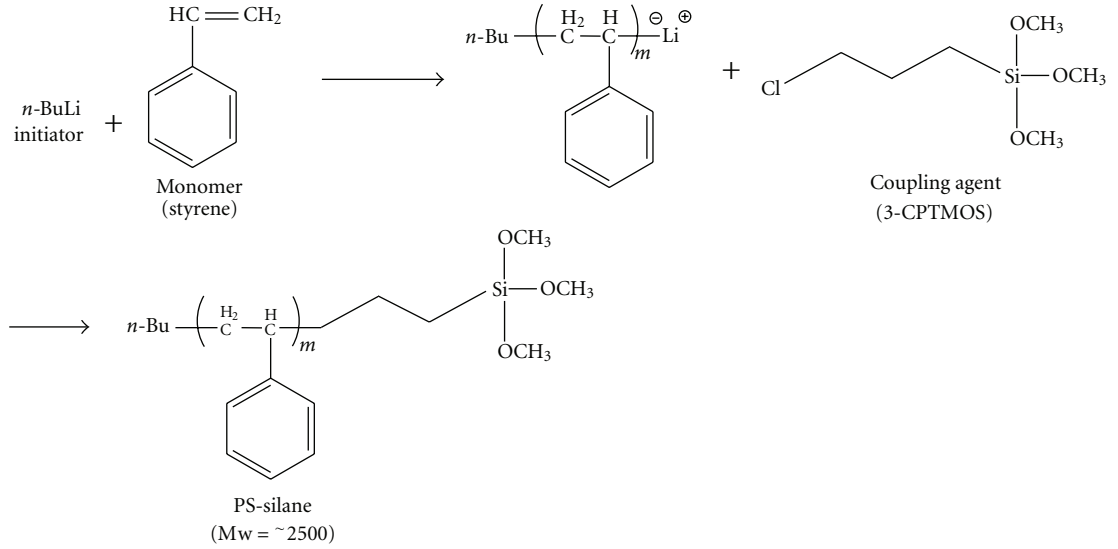

Scheme 1: Synthesis of PS-silane.

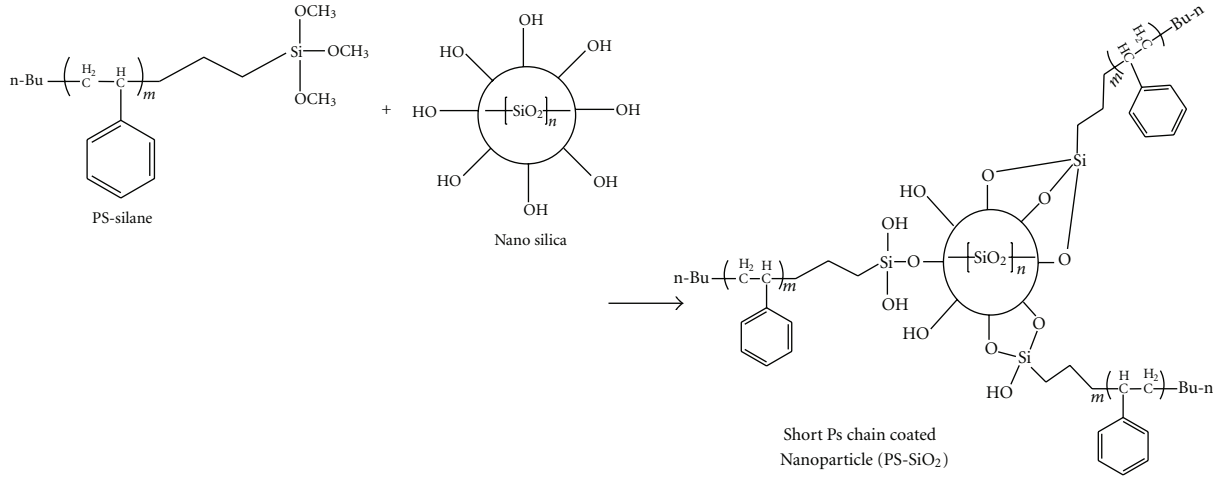

Scheme 2: Synthesis of PS-SiO_2.

organic-inorganic nanocomposite material with a targeted PS/PMMA volume ratios. We envisioned that the compatibility between PS-SiO_2 and the PS-*b*-PMMA would result in a dispersion of SiO_2 nanoparticles exclusively in the PS microdomain and thus enable a uniform distribution of the inorganic SiO_2 particles in the organic polymeric matrix.

2. Experimental

2.1. Materials. Styrene (S) and methyl methacrylate (MMA) (both with a purity of 99%) were acquired from Aldrich and predistilled with CaH_2 to remove the inhibitor before use. *n*-Butyllithium (n-*BuLi*) was obtained from Taiwan Synthetic Rubber Corp. 1,1-Diphenyethylene (DPE) purchased from Alfa Aesar had a purity of 98% and was diluted in toluene at a concentration of 0.6M before use. (3-Chloropropyl) trimethoxysilane (3-CPTMOS) was acquired from Aldrich at 97% purity. Colloidal nanosized silica (SiO_2) of a diameter of 10~20 nm was supplied by Echo Nano-bio Co., Ltd., Taiwan as a clear suspension in isopropanol (IPA) with a solid content of 30%. Other chemicals were purchased from J. T. Baker and used as received.

2.2. Measurements. The molecular structures of PS-*b*-PMMA samples were determined from ^{1}HNMR (Varian-Unity INOVA-500 MHz) spectra of samples in deuterated chloroform ($CDCl_3$) at 30°C. The functional groups of samples were analyzed with a Shimadzu SSU-8000 FTIR spectrophotometer. Scanning electron microscope (SEM) images were obtained on a Hitachi S4800 Type I SEM system for samples spin-coated on a silicon wafer. The atomic force microscope (AFM) height-mode micrographs were obtained from the Quesant Universal SPM Instruments, using as the AFM tip a silicon nitride-based cantilever coated with a magnetic film.

Table 1: Molecular characteristics of PS-*b*-PMMA samples.

	Mol% of styrene	$Mw_{absolute}$ of PS	$Mw_{absolute}$ of PS-*b*-PMMA	Vol% of Styrene	PDI
Sample(1)	36.67	8655	23037	40.57	1.21
Sample(2)	25.53	17750	67535	28.79	1.26

(The absolute molecular weights of PS and PS-*b*-PMMA were measured by GPC and ^{1}HNMR, resp.).

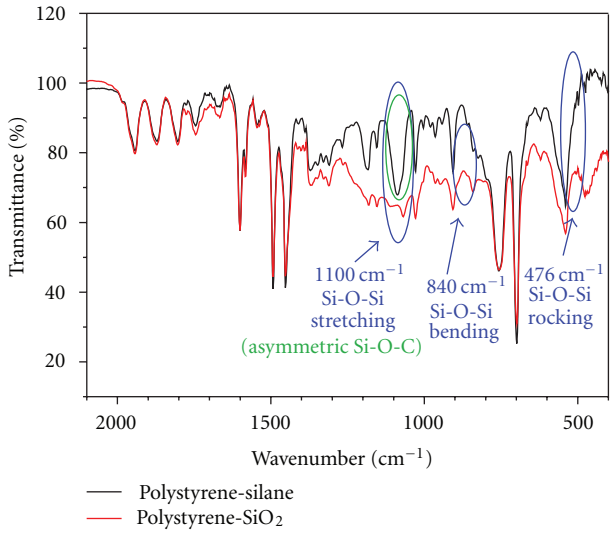

Figure 1: FTIR spectra for PS-silane and PS-SiO_2.

2.3. Synthesis and Characterization of PS-b-PMMA. The synthesis of PS-*b*-PMMA was accomplished via a sequential anionic polymerization in toluene. The choice of toluene as the solvent was due to the need of a polar environment for the polymerization of MMA. The PS-*b*-PMMA was synthesized following typical anionic polymerization procedures [39, 40]. A total of 150 mL of toluene, 5 mL styrene monomer, and 0.2 mL of tetrahydrofuran (THF) (to accelerate the polymerization) were charged into a 250 mL pressure vessel under a slight nitrogen overpressure. Afterwards styrene was polymerized at room temperature for 1 hr with the addition of 0.202 mL n-*BuLi* as the initiator. The color turned to reddish orange indicating the presence of living polystyryllithium anions. Next, DPE was added, and the reaction continued for another 1 hr. Thus, the living PS chain was capped by the DPE molecule (or a few DPE molecules) so as to provide the steric hindrance required for the following MMA polymerization. Thereafter, the reactor temperature was lower to −78°C, and 4 mL of MMA monomer was added to continue the polymerization reaction for 1 hr, forming the final product PS-*b*-PMMA. The low polymerization temperature, that is, −78°C, was necessary in order to minimize the unwanted side reactions. At the completion of the reaction, methanol was added to quench the reaction and the vessel content was poured into a large amount of deionized water under vigorous stirring to extract residual salts into the aqueous phase. The organic phase containing the dissolved PS-*b*-PMMA was then separated from the aqueous phase. The extraction step was repeated three times, and the final organic phase was poured into methanol for the precipitation of PS-*b*-PMMA. The precipitated PS-*b*-PMMA was then dried at 40°C in a vacuum. The control of the block lengths of PS-*b*-PMMA has been achieved by the precise control of the feed amount of styrene and MMA.

2.4. Synthesis and Characterization of PS-Silane. In order to blend the hydrophilic SiO_2 into PS-*b*-PMMA matrix, PS-silane was first prepared via Scheme 1.

A total of 100 mL cyclohexane, 0.2 mL THF, and 5 mL styrene monomer was charged into a 250 mL glass reactor, followed by the addition of 2 mL n-*BuLi*. The reaction was allowed to proceed for 1 hr before termination with 3-CPTMOS. The PS-silane was precipitated in methanol and dried. A low molecular weight PS (MW = 2200, PDI = 1.10) was synthesized by controlling the ratio of n-*BuLi* to styrene. At the end of polymerization, 3-CPTMOS was added to terminate the living PS chain forming the PS-silane.

2.5. Functionalization of SiO_2 by Anchoring PS-Silane onto Nanosilica via the Sol-Gel Reaction to (Making PS-SiO_2). The hydrophilic nanosilica particles contain inherent hydroxyls at the surface and can hardly react with the hydrophobic PS-silane. Fortunately, a mixture of dichlorobenzene (DCB) and IPA at 3 : 2 volume ratio is able to dissolve both of them. Thus, the sol-gel reaction occurs (with an addition of 0.1 M HCl to maintain the pH at 3 ~ 4) between the nanosilica and PS-silane in the mixed solvent as in Scheme 2.

In this work, a total of 0.5 g of PS-silane was dissolved in 15 g of DCB followed by the addition of 10 g of IPA and 0.09 g of 30 wt% SiO_2 in IPA solution. The mixture was agitated at 75°C for 3 mins, and then 2 g of 0.1 M HCl was added. The sol-gel reaction was allowed to take place for 2 hrs before the PS-SiO_2 was precipitated out in methanol.

2.6. Blending of PS-b-PMMA with PS-SiO_2 to Make a Hybrid Film. PS-*b*-PMMA and PS-SiO_2 were mixed at various weight ratios in toluene for preparing a solution of 1 wt% concentration. Afterwards, 9 drops of solution were added onto the surface of a 2 cm × 2 cm wafer which had been cleaned with acetone, IPA, and deionized water sequentially and dried before use. The hybrid film was made after 60 sec spin coating at 4000 rpm. Thereafter, the wafer was put together with the film in a vacuum oven at 180°C for annealing and self-assembling. After 24 hrs, the temperature was lowered to 30°C, and the drying continued for another 24 hrs.

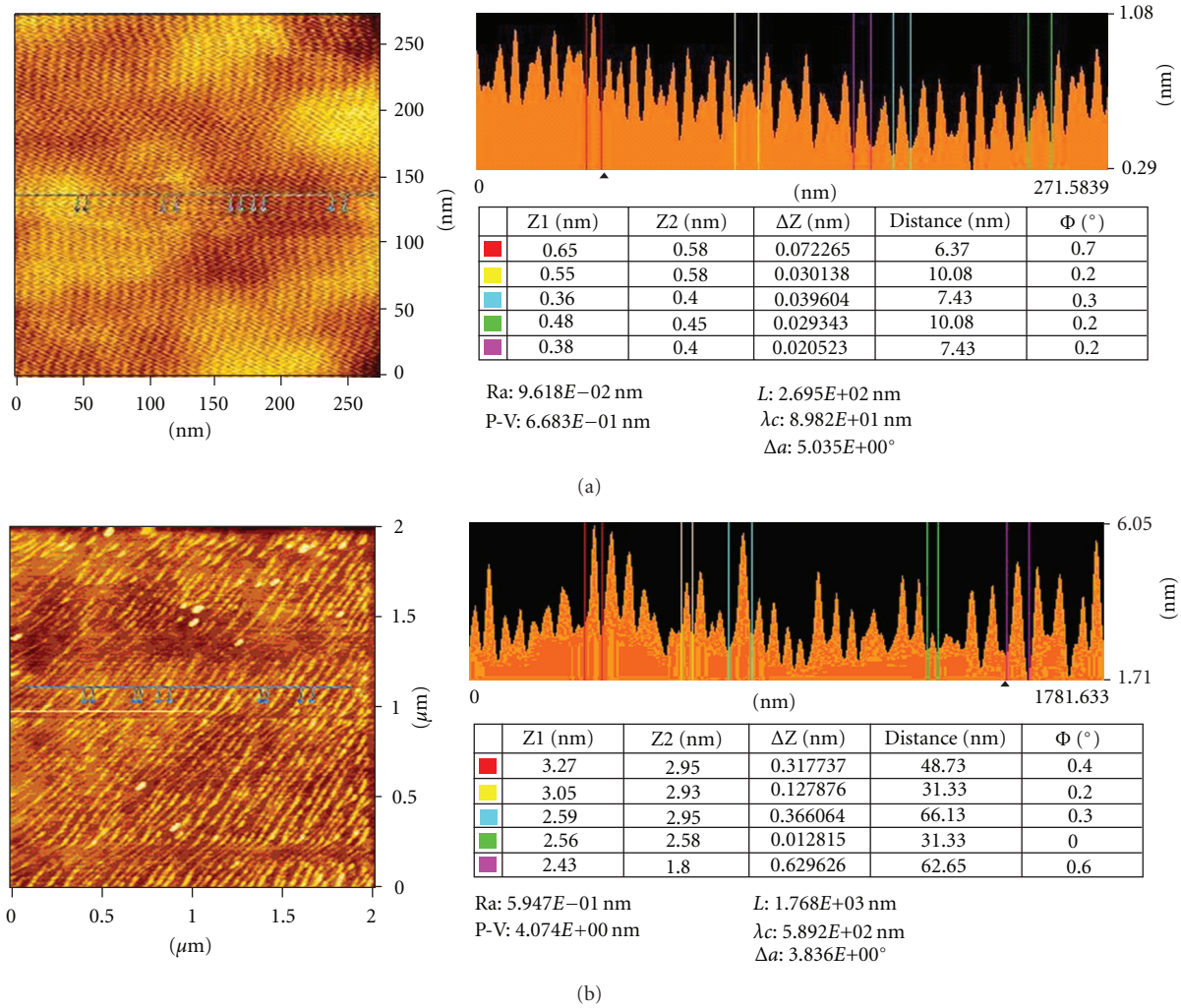

	Z1 (nm)	Z2 (nm)	ΔZ (nm)	Distance (nm)	Φ (°)
■	0.65	0.58	0.072265	6.37	0.7
■	0.55	0.58	0.030138	10.08	0.2
■	0.36	0.4	0.039604	7.43	0.3
■	0.48	0.45	0.029343	10.08	0.2
■	0.38	0.4	0.020523	7.43	0.2

Ra: 9.618E−02 nm
P-V: 6.683E−01 nm

L: 2.695E+02 nm
λc: 8.982E+01 nm
Δa: 5.035E+00°

(a)

	Z1 (nm)	Z2 (nm)	ΔZ (nm)	Distance (nm)	Φ (°)
■	3.27	2.95	0.317737	48.73	0.4
■	3.05	2.93	0.127876	31.33	0.2
■	2.59	2.95	0.366064	66.13	0.3
■	2.56	2.58	0.012815	31.33	0
■	2.43	1.8	0.629626	62.65	0.6

Ra: 5.947E−01 nm
P-V: 4.074E+00 nm

L: 1.768E+03 nm
λc: 5.892E+02 nm
Δa: 3.836E+00°

(b)

Figure 2: (a) AFM image of sample(1), and (b) AFM image of sample(1)/PS-SiO_2.

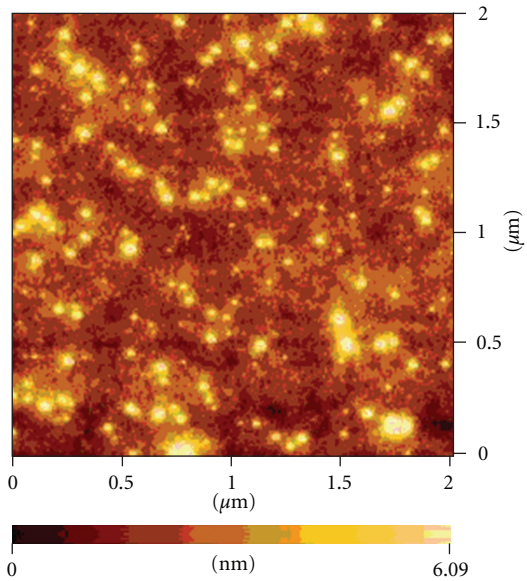

Figure 3: AFM image of sample(1)/PS-SiO_2 with 7 : 3 volume ratio of PS to PMMA.

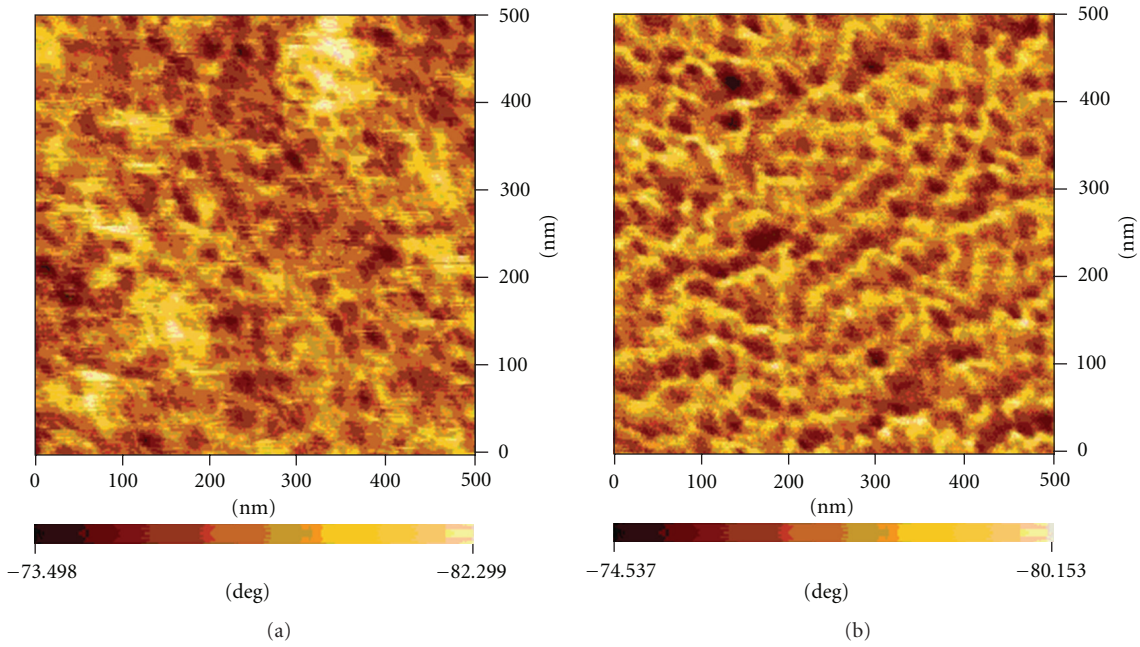

Figure 4: (a) AFM image of sample(2), and (b) AFM image of sample(2)/PS-SiO_2 with 5 : 5 volume ratio of PS to PMMA.

3. Results and Discussion

Two, PS-*b*-PMMA samples have been synthesized in this work and the polymers are characterized by GPC(SEC) and ^{1}HNMR as shown in Table 1. Based on the measured molecular weights of PS block and PS-*b*-PMMA, the molecular weight of PMMA block is calculated. Afterwards, the volume fraction of PS and PMMA blocks are calculated by dividing the molecular weights of each block by the well-known density of corresponding PS and PMMA homopolymer, ρ_{PS} (= 1.05 g/cm^3) and ρ_{PMMA} (= 1.19 g/cm^3).

The synthesized PS-silane has been verified by GPC and ^{1}HNMR to have a molecular weight of 2363 (PDI: 1.10) which comprises a PS chain length of 2200 and a terminal 3-CPTMOS (molecular weight: 163 after the elimination of chlorine atom).

The successful completion of the sol-gel reaction between PS-silane and SiO_2 has been verified by the disappearance of Si-O-C stretches and the generation of Si-O-Si stretches in the PS-SiO_2 spectrum (as shown in Figure 1).

While the sol-gel reaction occurs between PS-silane and the nanosilica particle, sol-gel reaction can also occur between nanosilica particles owing to the silanol groups on the surface of these particles. As a result, it is difficult either to analyze the number of PS-silane molecules bound to each nanosilica particle or to achieve a uniform size of the final PS-SiO_2 particles. Nevertheless, despite a few aggregates, the particle size of PS-SiO_2 observed under AFM is largely within a range of 15 ~ 40 nm. Blending various amounts of these PS-SiO_2 particles into the aforementioned PS-*b*-PMMA samples enables us to make composite materials with various PS to PMMA ratios, which indirectly affects the morphologies. All samples, either the pristine PS-*b*-PMMA or the PS-*b*-PMMA/PS-SiO_2 composites, after being spin-coated as films on silicon wafer and annealed at 180°C for 24 hrs, were examined under AFM. The AFM image of sample(1), having a nearly 4 : 6 PS/PMMA volume ratio, exhibits phase separation of a lamellar type (shown in Figure 2(a)). The size of each microdomain (either PS or PMMA layer thickness) is approximately 6–10 nm. In contrast, the composite, comprising 0.018 g of PS-SiO_2 and 0.1 g of sample(1), has a 5 : 5 volume ratio and displays a markedly different phase morphology (shown in Figure 2(b)).

In these AFM images, the bright yellow layers represent the PMMA microdomains, the dark brown areas represent the PS microdomains, and the bright spots represent SiO_2 particles. Because the PS-SiO_2 particles are compatible with the PS microdomain of sample(1), they tend to reside in the PS microdomain. However, because the size of PS-SiO_2 particles (15 ~ 40 nm) is larger than the microdomain size of sample(1) (6–10 nm), PS-SiO_2 particles has enlarged the PS microdomain and caused a rearrangement of PMMA microdomains. Because the size of the PMMA microdomain has been measured as 30 ~ 70 nm, the incorporation of PS-SiO_2 into the PS microdomain thereby has also enlarged the size of the PMMA microdomain.

Furthermore, when sample(1) is blended with PS-SiO_2 to make a composite with 7 : 3 PS to PMMA volume ratio, the number of bright spots increases as a result of an increase in the amount of PS-SiO_2 (Figure 3). It is worthy to note that the phase separation which used to be seen clearly in sample(1) now disappears. Apparently, the excessive amount of PS-SiO_2 poses an extreme constraint on the molecular rearrangement and makes the microdomain separation unobservable.

Similar investigations have been conducted on sample (2). At a nearly 3 : 7 PS to PMMA volume ratio, sample(2) exhibits a cylindrical morphology for PS microdomain

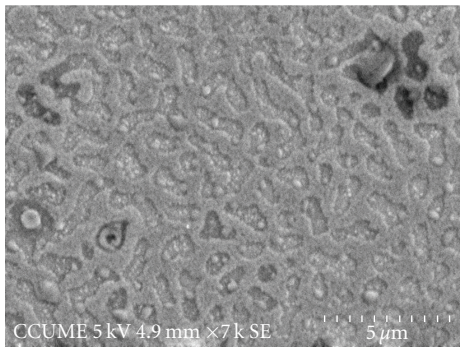

Figure 5: SEM micrograph of sample(2)/PS-SiO_2 at 5 : 5 PS/PMMA volume ratio.

oriented in either the vertical or the horizontal direction (shown in Figure 4(a)). The size of the PS microdomain is approximately 20–30 nm.

0.1 g of sample(2) has also been blended with 0.039 g of PS-SiO_2, that is, 39% addition, to make a composite sample with a 5 : 5 PS to PMMA volume ratio. Because the PS microdomain size is larger than the particle size of PS-SiO_2, it is theoretically easier to have all the PS-SiO_2 particles embedded in the PS microdomain during the blending of PS-SiO_2 with PS-*b*-PMMA. Therefore, it would be difficult to distinguish the SiO_2 particles from the PS microdomains (as shown in Figure 4(b)). In order to observe the distribution of PS-SiO_2 particles and examine whether there is any microdomain changes after the blending of PS-SiO_2 with PS-*b*-PMMA, SEM has been used. The SEM micrograph for a composite sample with a 5 : 5 PS to PMMA volume ratio is shown in Figure 5.

Owing to the indistinguishable electron densities of PS and PMMA, RuO_4 has been used for the dyeing of PS microdomain to facilitate the microscopy analysis [41–43]. It is clearly seen that all PS-SiO_2 particles are selectively residing in the islanded PS microdomains and the PS microdomains are enlarged by the incorporation of PS-SiO_2 particles (presumably caused by the molecular chain rearrangement during the domain formation). Furthermore, the incorporation of PS-SiO_2 particles also transforms the morphology from cylinders to islanded bicontinuous microstructures because of the inherent low surface energy of SiO_2.

4. Conclusion

With PS-tethering, SiO_2 nanoparticles can be dispersed selectively in the PS microdomain of PS-*b*-PMMA block copolymer. Despite the change in size and morphology of microdomains, the uniform distribution of the PS microdomain in the PS-*b*-PMMA polymer enables us to achieve a uniform distribution of the inorganic SiO_2 particles in the organic polymeric matrix.

Acknowledgment

Financial support provided by the National Science Council of the Republic of China under the program NSC97-2221-E-194-002-MY3 is greatly appreciated.

References

[1] F. S. Bates, "Polymer-polymer phase behavior," *Science*, vol. 251, no. 4996, pp. 898–905, 1991.

[2] E. L. Thomas, "The ABCs of self-assembly," *Science*, vol. 286, no. 5443, p. 1307, 1999.

[3] L. Zhu, S. Z. D. Cheng, P. Huang et al., "Nanoconfined polymer crystallization in the hexagonally perforated layers of a self-assembled PS-b-PEO diblock copolymer," *Advanced Materials*, vol. 14, no. 1, pp. 31–34, 2002.

[4] S. Choi, K. M. Lee, C. D. Han, N. Sota, and T. Hashimoto, "Phase transitions in sphere-forming polystyrene-block-polyisoprene-block-polystyrene copolymer and its blends with homopolymer," *Macromolecules*, vol. 36, no. 3, pp. 793–803, 2003.

[5] E. Buck and J. Fuhrmann, "Surface-induced microphase separation in spin-cast ultrathin diblock copolymer films on silicon substrate before and after annealing," *Macromolecules*, vol. 34, no. 7, pp. 2172–2178, 2001.

[6] Y. L. Loo, R. A. Register, and A. J. Ryan, "Modes of crystallization in block copolymer microdomains: breakout, templated, and confined," *Macromolecules*, vol. 35, no. 6, pp. 2365–2374, 2002.

[7] Y. L. Loo, R. A. Register, A. J. Ryan, and G. T. Dee, "Polymer crystallization confined in one, two, or three dimensions," *Macromolecules*, vol. 34, no. 26, pp. 8968–8977, 2001.

[8] A. Röttele, T. Thurn-Albrecht, J. U. Sommer, and G. Reiter, "Thermodynamics of formation, reorganization, and melting of confined nanometer-sized polymer crystals," *Macromolecules*, vol. 36, no. 4, pp. 1257–1260, 2003.

[9] C. C. Weng and K. H. Wei, "Selective distribution of surface-modified TiO_2 nanoparticles in polystyrene-b-poly (methyl methacrylate) diblock copolymer," *Chemistry of Materials*, vol. 15, no. 15, pp. 2936–2941, 2003.

[10] Y. Fink, A. M. Urbas, M. G. Bawendi, J. D. Joannopoulos, and E. L. J. Thomas, "Block copolymers as photonic bandgap materials," *Journal of Lightwave Technology*, vol. 17, no. 11, pp. 1963–1969, 1999.

[11] A. C. Edrington, A. M. Urbas, P. DeRege et al., "Polymer-based photonic crystals," *Advanced Materials*, vol. 13, no. 6, pp. 421–425, 2001.

[12] S. W. Yeh, K. H. Wei, Y. S. Sun, U. S. Jeng, and K. S. Liang, "Morphological transformation of PS-b-PEO diblock copolymer by selectively dispersed colloidal CdS quantum dots," *Macromolecules*, vol. 36, no. 21, pp. 7903–7907, 2003.

[13] B. J. Kim, J. J. Chiu, G. R. Yi, D. J. Pine, and E. J. Kramer, "Nanoparticle-induced phase transitions in diblock-copolymer films," *Advanced Materials*, vol. 17, no. 21, pp. 2618–2622, 2005.

[14] S. C. Park, B. J. Kim, C. J. Hawker, E. J. Kramer, J. Bang, and J. S. Ha, "Controlled ordering of block copolymer thin films by the addition of hydrophilic nanoparticles," *Macromolecules*, vol. 40, no. 22, pp. 8119–8124, 2007.

[15] C. P. Li, C. H. Wu, K. H. Wei et al., "The effect of nanoscale confinement on the collective electron transport behavior in au nanoparticles self-assembled in a nanostructured polystyrene-block-poly(4-vinylpyridine) diblock copolymer ultrathin film," *Advanced Functional Materials*, vol. 17, no. 14, pp. 2283–2290, 2007.

[16] V. Z.-H. Chan, J. Hoffman, V. Y. Lee et al., "Ordered bicontinuous nanoporous and nanorelief ceramic films from serf assembling polymer precursors," *Science*, vol. 286, no. 5445, pp. 1716–1719, 1999.

[17] T. Hashimoto, K. Tsutsumi, and Y. Funaki, "Nanoprocessing based on bicontinuous microdomains of block copolymers: nanochannels coated with metals," *Langmuir*, vol. 13, no. 26, pp. 6869–6872, 1997.

[18] K. W. Ho, "Ozonation of hydrocarbon diene elastomers: a mechanistic study," *Journal of Polymer Science Part A: Polymer Chemistry*, vol. 24, no. 10, pp. 2467–2482, 2003.

[19] J. T. Goldbach, K. A. Lavery, J. Penelle, and T. P. Russell, "Nano- to macro-sized heterogeneities using cleavable diblock copolymers," *Macromolecules*, vol. 37, no. 25, pp. 9639–9645, 2004.

[20] K. W. Guarini, C. T. Black, and S. H. I. Yeung, "Optimization of diblock copolymer thin film self assembly," *Advanced Materials*, vol. 14, no. 18, pp. 1290–1294, 2002.

[21] E. Huang, P. Mansky, T. P. Russell et al., "Mixed lamellar films: evolution, commensurability effects, and preferential defect formation," *Macromolecules*, vol. 33, no. 1, pp. 80–88, 2000.

[22] E. Jeoung, T. H. Galow, J. Schotter et al., "Fabrication and characterization of nanoelectrode arrays formed via block copolymer self-assembly," *Langmuir*, vol. 17, no. 21, pp. 6396–6398, 2001.

[23] B. J. Melde, S. L. Burkett, T. Xu, J. T. Goldbach, T. P. Russell, and C. J. Hawker, "Silica nanostructures templated by oriented block copolymer thin films using pore-filling and selective-mineralization routes," *Chemistry of Materials*, vol. 17, no. 18, pp. 4743–4749, 2005.

[24] Q. Ren, H. J. Zhang, X. K. Zhang, and B. T. Huang, "Hydrogenated polybutadiene-polymethyl methacrylate (HPB-PMMA) block copolymer. I. Synthesis of polybutadiene-polymethyl methacrylate (PB-PMMA) block copolymer," *Journal of Polymer Science Part A: Polymer Chemistry*, vol. 31, no. 4, pp. 847–851, 1993.

[25] L. Rockford, S. G. J. Mochrie, and T. P. Russell, "Propagation of nanopatterned substrate templated ordering of block copolymers in thick films," *Macromolecules*, vol. 34, no. 5, pp. 1487–1492, 2001.

[26] T. Thurn-Albrecht, J. Schotter, G. A. Kästle et al., "Ultrahigh-density nanowire arrays grown in self-assembled diblock copolymers templates," *Science*, vol. 290, no. 5499, pp. 2126–2129, 2000.

[27] T. Thurn-Albrecht, R. Steiner, J. DeRouchey et al., "Nanoscopic templates from oriented block copolymer films," *Advanced Materials*, vol. 12, no. 11, pp. 787–791, 2000.

[28] S. Wei, B. Vaidya, A. B. Patel, S. A. Soper, and R. L. McCarley, "Photochemically patterned poly(methyl methacrylate) surfaces used in the fabrication of microanalytical devices," *Journal of Physical Chemistry B*, vol. 109, no. 35, pp. 16988–16996, 2005.

[29] J. O. Choi, J. A. Moore, J. C. Moore, J. C. Corelli, J. P. Silverman, and H. Bakhru, "Degradation of poly(methylmethacrylate) by deep ultraviolet, x-ray, electron beam, and proton beam irradiations," *Journal of Vacuum Science and Technology B: Microelectronics Processing and Phenomena*, vol. 6, no. 6, pp. 2286–2289, 1988.

[30] R. B. Fox, "Photodegradation of high polymers," in *Progress in Polymer Science*, A. D. Jenkins, Ed., pp. 47–89, Pergamon Press, London, UK, 1967.

[31] R. B. Fox, L. G. Isaacs, and S. Stokes, "Photolytic degradation of poly(methyl methacrylate)," *Journal of Polymer Science Part A: Polymer Chemistry*, vol. 1, no. 3, pp. 1079–1086, 1963.

[32] E. J. Harbron, V. P. McCaffrey, R. Xu, and M. D. E. Forbes, "Stereochemistry and pseudosymmetries in main chain polymeric free radicals," *Journal of the American Chemical Society*, vol. 122, no. 38, pp. 9182–9188, 2000.

[33] B. Rånby and J. F. Rabek, *Photodegradation, Photo-oxidation and Photostabilization of Polymers*, Wiley, London, UK, 1975.

[34] B. Rånby and J. F. Rabek, *ESR Spectroscopy in Polymer Research*, Springer-Verlag, Berlin, Germany, 1977.

[35] K. Kimishima, T. Hashimoto, and D. H. Chang, "Spatial distribution of added homopolymer within the microdomains of a mixture consisting of an ABA-type triblock copolymer and a homopolymer," *Macromolecules*, vol. 28, no. 11, pp. 3842–3853, 1995.

[36] K. I. Winey, E. L. Thomas, and L. J. Fetters, "Isothermal morphology diagrams for binary blends of diblock copolymer and homopolymer," *Macromolecules*, vol. 25, no. 10, pp. 2645–2650, 1992.

[37] R. J. Spontak, S. D. Smith, and A. Ashraf, "Linear multiblock copolymer/homopolymer blends of constant composition. 1. Low-molecular-weight homopolymers," *Macromolecules*, vol. 26, no. 19, pp. 5118–5124, 1993.

[38] N. Y. Vaidya, C. D. Han, D. Kim, N. Sakamoto, and T. Hashimoto, "Microdomain structures and phase transitions in binary blends consisting of a highly asymmetric block copolymer and a homopolymer," *Macromolecules*, vol. 34, no. 2, pp. 222–234, 2001.

[39] H. Hückstädt, V. Abetz, and R. Stadler, "Synthesis of a polystyrene-arm -polybutadiene-arm-poly(methyl methacrylate) triarm star copolymer," *Macromolecular Rapid Communications*, vol. 17, no. 8, pp. 599–606, 1996.

[40] K. Sugiyama, T. Oie, A. A. Ei-Magd, and A. Hirao, "Synthesis of well-defined (AB)n multiblock copolymers composed of polystyrene and poly(methyl methacrylate) segments using specially designed living AB diblock copolymer anion," *Macromolecules*, vol. 43, no. 3, pp. 1403–1410, 2010.

[41] Y. Sun, M. Steinhart, D. Zschech, R. Adhikari, G. H. Michler, and U. Gösele, "Diameter-dependence of the morphology of PS-b-PMMA nanorods confined within ordered porous alumina templates," *Macromolecular Rapid Communications*, vol. 26, no. 5, pp. 369–375, 2005.

[42] T. M. Chou, P. Prayoonthong, A. Aitouchen, and M. Libera, "Nanoscale artifacts in RuO4-stained poly(styrene)," *Polymer*, vol. 43, no. 7, pp. 2085–2088, 2002.

[43] B. Ohlsson and B. Törnell, "Use of RuO4 in studies of polymer blends by scanning electron microscopy," *Journal of Applied Polymer Science*, vol. 41, no. 5-6, pp. 1189–1196, 1990.